

Hot Spots and Transition from d-Wave to Another Pairing Symmetry in the Electron-Doped Cuprate Superconductors

V. A. Khotel,^{1,2} Victor M. Yakovenko,² M. V. Zverev,³ and Haeyong Kang^{4,2}

¹Russian Research Centre Kurchatov Institute, Moscow 123182, Russia

²Condensed Matter Theory Center and Center for Superconductivity Research, Department of Physics, University of Maryland, College Park, Maryland 20742-4111, USA

³Russian Research Centre Kurchatov Institute, Moscow, 123182, Russia

⁴Department of Physics, Ewha Womans University, Seoul 120-750, South Korea

(Dated: cond-mat/0307454, v.1: 17 July 2003, v.2: 4 December 2003, v.3: 13 March 2004)

We present a simple theoretical explanation for a transition from d-wave to another superconducting pairing observed in the electron-doped cuprates. The $d_{x^2-y^2}$ pairing potential, which has the maximal magnitude and opposite signs at the hot spots on the Fermi surface, becomes suppressed with the increase of electron doping, because the hot spots approach the Brillouin zone diagonals, where $d_{x^2-y^2}$ vanishes. Then, $d_{x^2-y^2}$ pairing is replaced by either singlet s-wave or triplet p-wave pairing. We argue in favor of the latter and propose experiments to uncover it.

PACS numbers: 74.72.-h, 74.20.Rp, 74.20.Mn

I. INTRODUCTION

The superconducting pairing symmetry in the electron-doped cuprates [1], such as $\text{Nd}_{2-x}\text{Ce}_x\text{CuO}_4$ and $\text{Pr}_{2-x}\text{Ce}_x\text{CuO}_4$, has been debated for a long time. Originally, it was thought to be of the s-wave type [2]. Later, observation of the half-quantum magnetic flux in tricrystals [3], improved microwave measurements of temperature dependence of the London penetration depth [4], the angular-resolved photoemission spectroscopy (ARPES) [5] and Raman scattering [6] studies, and observation of the H dependence of specific heat on magnetic field H [7] pointed to the d-wave symmetry. Recently, evidence was found for a transition from d- to s-wave pairing symmetry with the increase of electron doping [8, 9]. Biswas et al. [8] concluded that $\text{Pr}_{2-x}\text{Ce}_x\text{CuO}_4$ has d-wave pairing at $x \leq 0.15$ and s-wave pairing at $x \geq 0.17$. In this paper, we propose a simple scenario for the transition from the d-wave to another pairing symmetry and argue that the latter can actually be triplet p-wave.

First we present a qualitative picture in terms of the Fermi surface geometry shown in Fig. 1. According to the theoretical model [10, 11, 12], the antiferromagnetic spin fluctuations (ASF) peaked at the wave vector $\mathbf{Q} = (\pi, \pi)$ are responsible for d-wave superconductivity in the hole-doped cuprates. Commensurate ASF at the wave vector \mathbf{Q} are also observed in the electron-doped cuprates [13]. The interaction via ASF has the highest strength at the so-called hot spots, the points on the Fermi surface connected to each other by the vector \mathbf{Q} . These points are labeled in Fig. 1 by the consecutive numbers from 1 to 8. Since the interaction via ASF is repulsive in the singlet channel, the superconducting pairing potential $\langle p \rangle$ has opposite signs at the two hot spots connected by the vector \mathbf{Q} :

$$\langle p + \mathbf{Q} \rangle = -\langle p \rangle: \quad (1)$$

Thus, the eight hot spots can be divided into four groups

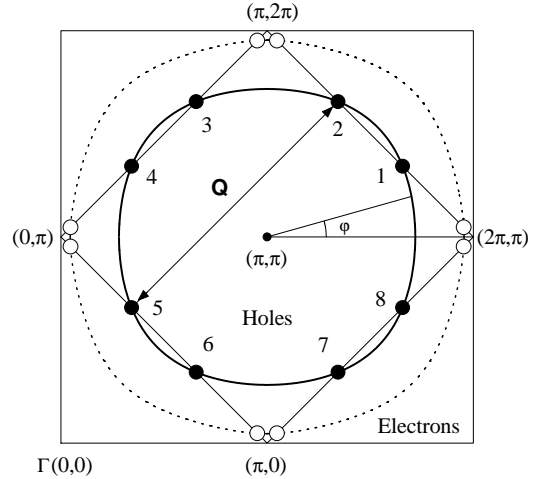


FIG. 1: Fermi surfaces of Eq. (2) for hole doping (dashed line, $x = 1/76$, $x = 0.48$) and electron doping (solid line, $x = 0.4$, $x = 0.15$). The hot spots are shown by open and solid circles. The radius of the circles $r = 0.1$ represents the width of the interaction (4) in the momentum space.

(1,6), (2,5), (3,8), and (4,7), with the signs of $\langle p \rangle$ being opposite within each group. However, the relative signs of $\langle p \rangle$ between the different groups have to be determined from additional considerations.

In Fig. 1, the dashed and solid lines show the Fermi surfaces corresponding to the hole- and electron-doped cuprates. Notice that the $\Gamma(0,0)$ point is located at the corner of Fig. 1, so that the area inside the Fermi surface is occupied by holes and outside by electrons. The dashed Fermi surface, corresponding to the hole-doped case, encloses a larger area, and the pairs of hot spots shown by the open circles in Fig. 1 are located close to the van Hove points $(0, \pm\pi)$, $(\pm\pi, 0)$, (π, π) , and $(\pi, -\pi)$. It is natural to assume that $\langle p \rangle$ has the same sign within each pair of the neighboring hot spots. This assumption,

in combination with Eq. (1), immediately results in the familiar $d_{x^2-y^2}$ symmetry of the pairing potential.

However, the situation does change in the electron-doped case. With the increase of electron doping, the Fermi surface shrinks, and the hot spots move away from the van Hove points toward the Brillouin zone diagonals. The following pairs of the hot spots approach each other: (1,2), (3,4), (5,6), and (7,8). The $d_{x^2-y^2}$ pairing potential has opposite signs within each pair and vanishes at the zone diagonals. Thus, in the electron-overdoped cuprates, when the hot spots get close enough, the $d_{x^2-y^2}$ pairing becomes suppressed. Then, a superconducting pairing of another symmetry may emerge, with the pairing potential of the same sign on both sides of the zone diagonals. This is the mechanism that we propose for the transition observed in Refs. [8, 9].

II. SUPPRESSION OF d-WAVE PAIRING

To illustrate how the $d_{x^2-y^2}$ pairing evolves with doping, we perform calculations employing the typical electron dispersion law

$$\epsilon(\mathbf{p}) = 2t_0 (\cos p_x + \cos p_y) + 4t_1 \cos p_x \cos p_y \quad (2)$$

with $t_1/t_0 = 0.45$. The chemical potential controls the hole concentration n , which is determined by the area S inside the Fermi surface in Fig. 1: $n = 2S/(2\pi)^2$. The doping $x = n - 1$ is defined as the deviation of n from half filling, so that $x > 0$ and $x < 0$ correspond to hole and electron doping [14]. The relation $S/(1+x)$ is in agreement with ARPES, except for the region of small doping around $x = 0$, where the antiferromagnetic Mott insulating state intervenes. For $\text{Nd}_{2-x}\text{Ce}_x\text{CuO}_4$, this was established in Ref. [15], and movement of hot spots toward the zone diagonals with the increase of electron doping was directly observed in Refs. [5, 15, 16]. Notice that, for the dispersion law (2), the hot spots exist only within a finite range of chemical potential

$4t_1 > \mu > 0$, which corresponds to the range of doping $0.25 = x_- < x < x_+ = 0.53$. The respective pairs of the hot spots merge and disappear at the van Hove points when $x \rightarrow x_+$ and at the zone diagonals when $x \rightarrow x_-$. Thus, in this model, the $d_{x^2-y^2}$ superconductivity can exist only within a finite range of electron and hole doping, in qualitative agreement with the experimental phase diagram of cuprates. Doping dependence of the Fermi surface in the electron-doped cuprates obtained from the ARPES measurements [5, 15, 16] was quantitatively interpreted within a simple band-structure model in Ref. [17]. The results are in qualitative agreement with the Hall coefficient measurements [18].

To verify the qualitative picture given in the Introduction, we solve the BCS equation for the pairing potential

$$\Delta(\mathbf{p}) = \frac{1}{V} \sum_{\mathbf{p}'} \Delta(\mathbf{p}') \frac{\tanh \frac{E(\mathbf{p}')}{2T}}{2E(\mathbf{p}')} - \Delta(\mathbf{p}) \frac{d^2 p^0}{(2\pi)^2} : \quad (3)$$

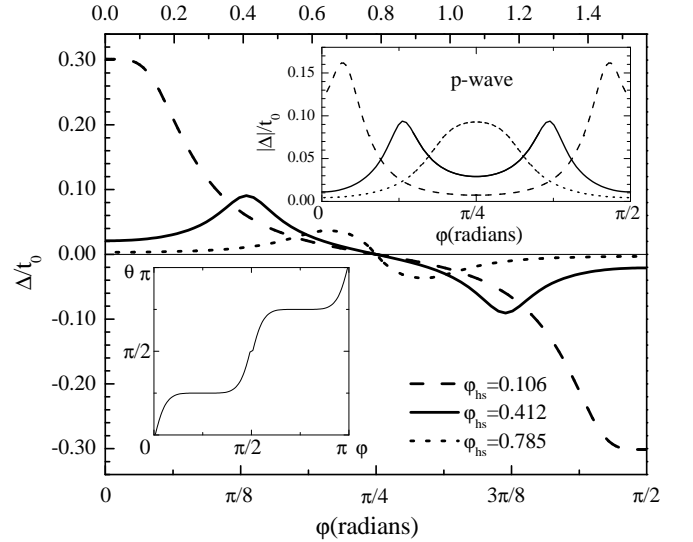


FIG. 2: The pairing potential Δ at $T = 0$ vs. the angle ϕ on the Fermi surface, shown by the dashed line for $x = 0.37$ ($\mu = 1.6t_0$), the solid line for $x = 0.1$ ($\mu = 0.6t_0$), and the dotted line for $x = 0.25$ ($\mu = 0$). The main panel represents the $d_{x^2-y^2}$ state, and the upper inset the chiral p-wave state. The angle ϕ_{hs} indicates position of the hot spot 1. The lower inset shows the phase θ of $\Delta = |\Delta|e^{i\theta}$ for the chiral p-wave pairing.

Here $E(\mathbf{p}) = \sqrt{V_c^2(\mathbf{p}) + V_s^2(\mathbf{p})}$, T is temperature, and $V(\mathbf{q}) = V_c(\mathbf{q}) + V_s(\mathbf{q})$ is the effective interaction between electron charges and spins, where $\sigma_x, \sigma_y, \sigma_z$ are the Pauli matrices, and \uparrow, \downarrow are the spin indices. For singlet and triplet pairings, the functions $V_0(\mathbf{q}) = V_c(\mathbf{q}) - 3V_s(\mathbf{q})$ and $V_1(\mathbf{q}) = V_c(\mathbf{q}) + V_s(\mathbf{q})$ enter Eq. (3), respectively. To simplify our calculations, we ignore the frequency dependence of V and use the conventional ASF interaction of the form [11]

$$V_0(\mathbf{q}) = \frac{g}{(q - Q)^2 + \gamma^2} \quad (4)$$

with the coupling constant $g = 2t_0$ and the width $\gamma = 0.1$ [19].

The $d_{x^2-y^2}$ pairing potential Δ , calculated at $T = 0$ for three different dopings, is shown in the main panel of Fig. 2 vs. the angle ϕ on the Fermi surface (see Fig. 1). The dashed line refers to the strong hole doping $x = 0.37$ close to x_+ , the dotted line to the strong electron doping $x = x_- = 0.25$, and the solid line to the intermediate electron doping $x = 0.1$. The angle ϕ_{hs} indicates the position of the hot spot 1 for these dopings. We see that the maxima of $|\Delta(\phi)|$ are achieved at the hot spots, i.e. at $\phi = \phi_{hs}$, as discussed in Ref. [20]. The solid curve in Fig. 2 qualitatively agrees with the nonmonotonic function $|\Delta(\phi)|$ inferred from the Raman scattering in $\text{Nd}_{1.85}\text{Ce}_{0.15}\text{CuO}_4$ [6]. We also observe that $|\Delta|$ drops precipitously when the hot spots approach the zone diagonals. This happens because the integral in Eq. (3) is suppressed when positive and negative peaks of $\Delta(\phi)$ are

close to each other.

III. ALTERNATIVE SUPERCONDUCTING PAIRINGS

Once the $d_{x^2-y^2}$ pairing is suppressed in the case of strong electron doping, pairing of a different symmetry may emerge in the system. Evidently, this pairing should provide the same sign of Δ within each pair (1,2), (3,4), (5,6), and (7,8) of the approaching hot spots. There are three possibilities depending on the relative signs of Δ between the different pairs of the hot spots. The same sign for all the hot spots corresponds to s-wave, the opposite sign between (1,2) and (3,4) to d_{xy} -wave, and the opposite sign between (1,2) and (5,6) to triplet p-wave pairing. We need to find out which of these states wins.

Measurements of the temperature dependence of the penetration depth $\lambda(T)$ show a transition from a gap with nodes to a nodeless gap with the increase of electron doping in $\text{Pr}_{1-x}\text{Ce}_x\text{CuO}_4$ and $\text{La}_{2-x}\text{Ce}_x\text{CuO}_{4-y}$ [9]. The point contact spectroscopy of $\text{Pr}_{1-x}\text{Ce}_x\text{CuO}_4$ [8] shows a transition from a strong zero-bias conductance peak, originating from the midgap Andreev surface states in the d-wave case, to double peaks typical for s-wave. These experiments eliminate d_{xy} -wave pairing, because it has gap nodes and the midgap Andreev states. d_{xy} -wave pairing was proposed in Ref. [21] as a possible successor to $d_{x^2-y^2}$ in the electron-overdoped phase. In the theoretical model of Ref. [21], nonlocal corrections to the Hubbard interaction U due to spin fluctuations were taken into account only in the lowest order in U , whereas in our model (4) the peak at Q is obtained by summing an infinite number of RPA-like diagrams. The interaction (4) peaked at $Q = (\pi, \pi)$ is not favorable for d_{xy} -wave pairing.

The simplest alternative pairing symmetry consistent with the experiments [8, 9] is s-wave, which can be produced by phonons. This scenario was proposed by Abrikosov [22], who argued that, with the increase of doping, d-wave superconductivity is destroyed by disorder, whereas s-wave superconductivity survives. The s-wave energy gap Δ has no nodes and is roughly uniform along the Fermi surface. However, the s-wave scenario encounters some problems. When $\Delta(\mathbf{p})$ varies along the Fermi surface, measurements of $\lambda(T)$ yield the minimal value of the gap Δ_{\min} at $T = 0$. The experiment [23] found $\Delta_{\min}/T_c = 0.85$, whereas, for the phonon-induced s-wave superconductivity, this ratio should be close to the BCS value 1.76. Furthermore, for the phonon mechanism, T_c is not expected to depend on doping significantly [22], whereas the experimental T_c declines steeply at $x > 0.15$ and vanishes for $x > 0.2$ outside of the dome-shaped phase diagram of the electron-doped cuprates [1, 24]. Incidentally, the value of doping where superconductivity disappears is close to x_c , which indicates that the hot spots may be equally important for the alternative superconducting pairing.

Thus, it is worth considering the last alternative pairing, namely the triplet p-wave. It has the order parameter $\Delta = \Delta_0 \mathbf{n}$, where \mathbf{n} is the antisymmetric spin tensor, and \mathbf{n} is the unit vector of spin-polarization [25]. The symmetry of triplet pairing in a tetragonal crystal was classified in Ref. [26]. In the E_g representation, \mathbf{n} points along the c axis, and the phase of $\Delta(\mathbf{p})$ changes by 2π around the Fermi surface. This order parameter is chiral and breaks the time-reversal symmetry. The simplest example is $\Delta(\mathbf{p}) = \Delta_0 (\sin p_x - i \sin p_y)$, which was originally proposed for Sr_2RuO_4 [27]. In the A_{1u} , A_{2u} , B_{1u} , and B_{2u} representations, the vector \mathbf{n} lies in the (a,b) plane and rotates around the Fermi surface by the angle 2π . These order parameters are not chiral and do not break the time-reversal symmetry. Both types of the pairing potential have two components $(\Delta_1; \Delta_2)$, the real and imaginary parts of Δ in the chiral case and $(n_x; n_y)$ in the nonchiral case, which satisfy the symmetry relation $j_2(p_x; p_y)\Delta = j_1(p_y; p_x)\Delta$. Then, the gap $\Delta = \Delta_1 + i\Delta_2$ does not have nodes, but is modulated along the Fermi surface. This easily explains the reduced value of Δ_{\min}/T_c observed in Ref. [23]. The tunneling spectrum, shown in Fig. 3 of Ref. [28] for $\Delta(\mathbf{p}) = \Delta_0 (\sin p_x - i \sin p_y)$, has double peaks, as in the experiment [8]. Thus, the experiments [8, 9, 23] are compatible with both s- and p-wave pairings and are not sufficient to distinguish between them.

Measurements of the Knight shift can distinguish between singlet and triplet pairing. The Knight shift in the electron-doped $\text{Pr}_{0.91}\text{LaCe}_{0.09}\text{CuO}_{4-y}$ was found to decrease below T_c consistently with the singlet d-wave pairing [29]. However, the Knight shift in $\text{Pr}_{1.85}\text{Ce}_{0.15}\text{CuO}_{4-y}$ was found not to change below T_c [30]. This is an indication of triplet pairing, like in Sr_2RuO_4 [31] and in the organic superconductors $(\text{TM-TSF})_2\text{X}$ [32]. To obtain a complete picture, it is desirable to measure the Knight shift in the superconducting state systematically as a function of electron doping across the transition from $d_{x^2-y^2}$ pairing to a new pairing.

Spontaneous time-reversal-symmetry breaking in the chiral p-wave state can be detected by the muon spin-relaxation measurements [33] as in Sr_2RuO_4 [34], or by measuring the local magnetic field produced by the chiral Andreev surface states. Quantitative estimates done in Ref. [35] show that the latter effect can be realistically observed with a scanning SQUID microscope [36].

IV. COMPETITION BETWEEN d- AND p-WAVE PAIRINGS

As discussed after Eq. (3), the ASF interaction V_s enters in the singlet and triplet superconducting pairing channels with opposite signs. Thus, it is unfavorable for p-wave pairing, and a different mediator is needed. Triplet pairing is usually associated with the ferromagnetic spin fluctuations, e.g. in the superfluid He-3 [25] or

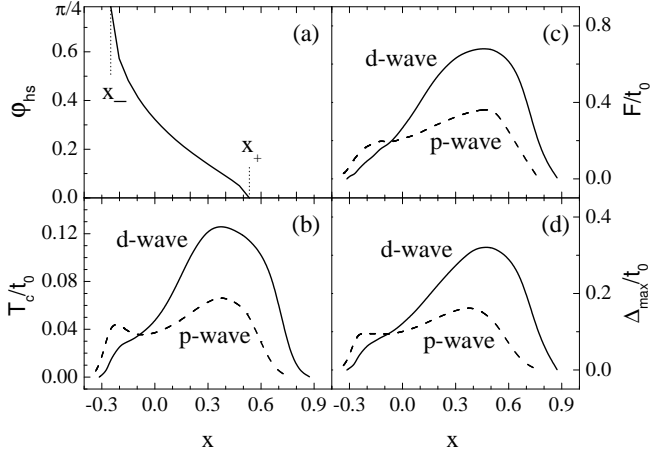


FIG. 3: Dependence of various quantities on doping x . Panel (a): the hot spot angle φ_{hs} , panel (b): the transition temperature T_c , panel (c): the condensation energy F , and panel (d): the maximum gap Δ_{max} . The solid and dashed lines correspond to the $d_{x^2-y^2}$ and to the chiral p-wave pairings.

Sr_2RuO_4 [37]. In Ref. [38], the symmetry of superconducting pairing was studied as a function of the Fermi surface change with doping in a square lattice model with nearest-neighbor interaction. It was found that the symmetry changes with doping from d-wave to p-wave to s-wave. The results were applied to Sr_2RuO_4 , but they may be also relevant to the electron-doped cuprates.

In the calculations given below, we focus on another possible mediator for p-wave pairing, namely the charge-density fluctuations (CDF) enhanced in the vicinity of the charge-density-wave (CDW) instability. The role of CDW fluctuations in cuprates was emphasized in Ref. [39]. In a crystal, the CDW wave vector is expected to be close to $Q = (\pi, \pi)$, and the CDF interaction $V_c(q)$ would have a peak at this vector. Such interaction has repulsive sign in the singlet and triplet particle-particle channels, resulting in the condition (1) and supporting both d- and p-wave superconducting pairings.

The relative strength of CDF vs. ASF in cuprates is subject to debate, and detailed evaluation of $V_c(q)$ is not the purpose of our paper [19]. Instead, we employ a toy model with the same interaction in the triplet and singlet channels: $V_1(q) = V_0(q) = V_c(q)$, where $V_c(q)$ is given by Eq. (4). Then, the difference in the solutions of the BCS equation (3) for d- and p-wave pairings results only from the geometry of the Fermi surface. The upper inset in Fig. 2 shows the magnitude $j(\theta)j$ and the lower inset the phase of $j(\theta) = j e^{i\theta}$ calculated for the chiral p-wave pairing. We observe that $j(\theta)j$ has maxima at the hot spots angles θ_{hs} , but, unlike in the $d_{x^2-y^2}$ case, it does not vanish at $\theta = \pi/4$ and is not suppressed when the hot spots approach the zone diagonals.

In Fig. 3, we show how various quantities depend on doping x . Panel (a) shows the hot spot angle φ_{hs} . Panels (b), (c), and (d) show the transition temperature T_c , the

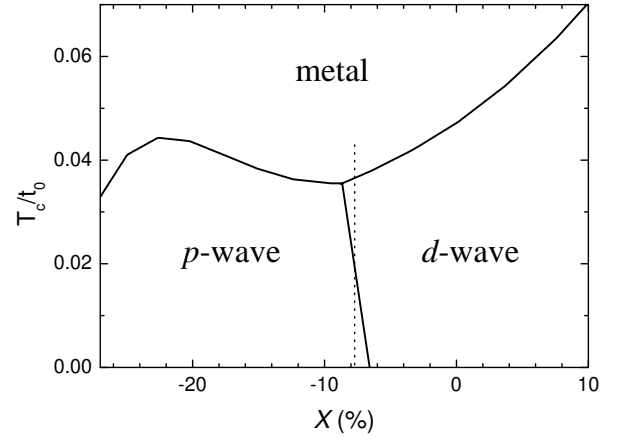


FIG. 4: Solid lines: Superconducting phase diagram of electron-doped cuprates vs. doping x calculated on the basis of Fig. 3. The vertical dashed line is a guide for eye.

maximum gap Δ_{max} , and the condensation energy F for the $d_{x^2-y^2}$ and chiral p-wave pairings. It is clear from Fig. 3 that, at the doping around $x \approx 8\%$, where the hot spots approach the zone diagonals closely enough, p-wave pairing wins over $d_{x^2-y^2}$ pairing. With further increase of electron doping beyond x_+ , hot spots disappear, and the proposed p-wave superconductivity rapidly vanishes, in qualitative agreement with the experimental phase diagram [1, 24]. It would be very interesting to verify this conjecture by ARPES measurements of the hot spots positions simultaneously with the superconducting phase diagram in the electron-overdoped regime.

Notice that the doping $x_1 = 8.8\%$, where the T_c curves for d- and p-waves cross in panel (b), is slightly different from the doping $x_2 = 6.6\%$, where the F curves cross in panel (c). This means that the critical dopings for the transition from d- to p-wave are slightly different at T_c and $T = 0$. Thus, the d-p transition line, obtained by connecting the transition points at T_c and $T = 0$, is not vertical, as shown in Fig. 4 by the solid line. If a sample has the doping x in between x_1 and x_2 , it should experience a transition from p-wave to d-wave with the increase of temperature, as shown in Fig. 4 by the dashed line. This effect was actually observed experimentally in the slightly overdoped samples of $\text{Pr}_{1.85}\text{Ce}_{0.15}\text{CuO}_4$ [41]. At low temperature, specific heat was found to depend linearly on a magnetic field H , indicating a fully-gapped pairing potential consistent with s- or p-wave. With the increase of temperature, the field dependence was found to change to H^2 , indicating a transition into d-wave state, as shown in Fig. 4.

In the simplest case, the d-p transition line in Fig. 4 is the first-order phase-transition line. Another possibility, calculated in Ref. [38], is that this line is split into two second-order phase-transition lines, and the p and d phases coexist in the intermediate region. Which of the two scenarios takes place is determined by the higher-order coefficients of the Landau expansion of the free en-

ergy (e.g. see discussion in Ref. [42]). Calculations of these coefficients depend on the details of a theoretical model and may be unreliable, e.g. they may be affected by renormalization [43]. Thus, the question of one first-order vs. two second-order transitions between d- and p-wave phases remains open, both theoretically and experimentally. We would like to point out that a similar question applies to a cascade of the magnetic-field-induced phase transitions in observed in organic conductors [42]. It was found experimentally [42] that in high magnetic fields the system exhibits single first-order phase transitions with hysteresis, whereas in lower fields it exhibits double-split second-order phase transitions without hysteresis. Thus, both scenarios can take place in the same sample under different conditions.

Positive x in Fig. 3 corresponds to hole doping. At $x = x_+$, the hot spots merge and disappear at the van Hove points $(0; \pi)$ and $(\pi; 0)$. Comparing panels (a) and (b) in Fig. 3, one may notice that the maximum of T_c is achieved at a hole doping $x < x_+$, and T_c rapidly decreases to zero for $x > x_+$. Naively one would expect maximal T_c at $x = x_+$, where the van Hove singularity is at the Fermi surface. However, the four hot spots surrounding each saddle point at $x < x_+$ cover more momentum space and, thus, produce a higher T_c than at $x = x_+$, where the four hot spots merge into one. These results are in qualitative agreement with the phase diagram of $\text{La}_{2-x}\text{Sr}_x\text{CuO}_4$ mapped to the ARPES measurements of its Fermi surface in Figs. 8 and 7 of Ref. [40]. In the experiment, the maximal T_c is achieved at $x = 15\%$, the Fermi surface passes through the van Hove points at $x = 22\%$, and T_c vanishes at $x = 27\%$. Our theoretical Fig. 3 shows the same sequence albeit at different values of x , because our dispersion law parameters t_0 and t_1 in Eq. (2) are not optimized for $\text{La}_{2-x}\text{Sr}_x\text{CuO}_4$.

V. CONCLUSIONS

We have shown that, when the hot spots approach the Brillouin zone diagonals in the electron-overdoped

cuprates, $d_{x^2-y^2}$ pairing becomes suppressed and is replaced by either singlet s-wave or triplet p-wave pairing. The transition is most likely of the first order as a function of doping x . To verify the proposed scenario, it is desirable to measure correlation between superconducting T_c and the hot spots positions by ARPES. We have given a number of arguments in favor of the triplet p-wave pairing, which may break the time-reversal symmetry. The Knight shift measurements in different samples of electron-doped cuprates show both singlet [29] and triplet [30] superconducting pairing, which may be an indication of the transition between the two types. Muon spin-relaxation and the scanning SQUID experiments can detect spontaneous violation of the time-reversal symmetry. Relationship between our proposed theoretical scenario of the superconducting symmetry change and the phenomenon of the electron dispersion law flattening is discussed in review [44].

Acknowledgments

VM Y thanks S.E. Brown and H. Balci for sharing their unpublished experimental results [30] and [41]. VAK and VM Y thank R.L. Greene for useful discussions, and the Kavli Institute for Theoretical Physics at Santa Barbara for the opportunity to start this collaboration. VAK and HK thank the Condensed Matter Theory Center for arranging their visits to the University of Maryland. VM Y is supported by the NSF Grant DMR-0137726, HK by the scholarship from Ewha Womans University and by Korean Research Foundation, VAK by the NSF Grant PHY-0140316 and by the McDonnell Center for Space Sciences, and VAK and MVZ by the Grant NS-18852003.2 from the Russian Ministry of Industry and Science.

Note added in proofs. Recently we became aware of Refs. [45] and [46], which studied evolution of d-wave superconductivity in the electron-doped cuprates.

-
- [1] H. Takagi, S. Uchida, and Y. Tokura, Phys. Rev. Lett. 62, 1197 (1989); Nature 337, 345 (1989).
 - [2] D. H. Wu, J. Mao, S. N. Mao, J. L. Peng, X. X. Xi, T. Venkatesan, R. L. Greene, and S. M. Anlage, Phys. Rev. Lett. 70, 85 (1993).
 - [3] C. C. Tsuei and J. R. Kirtley, Phys. Rev. Lett. 85, 182 (2000).
 - [4] J. D. Kokales, P. Fournier, L. V. Mercaldo, V. V. Talanov, R. L. Greene, and S. M. Anlage, Phys. Rev. Lett. 85, 3696 (2000); R. Prozorov, R. W. Giannetta, P. Fournier, and R. L. Greene, Phys. Rev. Lett. 85, 3700 (2000).
 - [5] N. P. Armitage, D. H. Lu, D. L. Feng, C. K. In, A. Damascelli, K. M. Shen, F. Ronning, Z.-X. Shen, Y. Onose, Y. Taguchi, and Y. Tokura, Phys. Rev. Lett. 86, 1126 (2001).
 - [6] G. Blumberg, A. Koitzsch, A. Gozar, B. S. Dennis, C. A. Kendziora, P. Fournier, and R. L. Greene, Phys. Rev. Lett. 88, 107002 (2002).
 - [7] H. Balci, V. N. Smolyaninova, P. Fournier, A. Biswas, and R. L. Greene, Phys. Rev. B 66, 174510 (2002).
 - [8] A. Biswas, P. Fournier, M. M. Qazilbash, V. N. Smolyaninova, H. Balci, and R. L. Greene, Phys. Rev. Lett. 88, 207004 (2002).
 - [9] J. A. Skinta, M. S. Kim, T. R. Lemberger, T. G. Reibe, and M. Naito, Phys. Rev. Lett. 88, 207005 (2002).
 - [10] D. J. Scalapino, E. Loh, Jr., and J. E. Hirsch, Phys. Rev. B 34, 8190 (1986); D. J. Scalapino, Phys. Rep. 250, 329

- (1995).
- [1] P. M. Onthoux, A. V. Balatsky, and D. Pines, Phys. Rev. Lett. 67, 3448 (1991); Phys. Rev. B 46, 14803 (1992).
 - [2] T. Mori, Y. Takahashi, and K. Ueda, J. Phys. Soc. Jpn. 59, 2905 (1990).
 - [3] K. Yamada, K. Kurauchi, T. Uefuji, M. Fujita, S. Park, S.-H. Lee, and Y. Endoh, Phys. Rev. Lett. 90, 137004 (2003).
 - [4] This definition of x is consistent with the doping parameter x in the chemical formulas, such as $\text{La}_{2-x}\text{Sr}_x\text{CuO}_4$.
 - [5] N. P. Armitage, F. Ronning, D. H. Lu, C. Kim, A. Damascelli, K. M. Shen, D. L. Feng, H. Eisaki, Z.-X. Shen, P. K. Mang, N. K. Aneko, M. G. Reven, Y. Onose, Y. Taguchi, and Y. Tokura, Phys. Rev. Lett. 88, 257001 (2002).
 - [6] N. P. Armitage, D. H. Lu, C. Kim, A. Damascelli, K. M. Shen, F. Ronning, D. L. Feng, P. Bogdanov, Z.-X. Shen, Y. Onose, Y. Taguchi, Y. Tokura, P. K. Mang, N. K. Aneko, and M. G. Reven, Phys. Rev. Lett. 87, 147003 (2001).
 - [7] C. Kusko, R. S. Markiewicz, M. Lindroos, and A. Bansil, Phys. Rev. B 66, 140513 (2002).
 - [8] Y. Dagan, M. M. Qazilbash, C. P. Hill, V. N. Kulkarni, and R. L. Greene, cond-mat/0310475.
 - [9] The purpose of our calculations is not to achieve precise numerical agreement with the experiment, but rather to illustrate how the proposed mechanism works within a simple model. The parameters of the model are not optimized for any particular material, and we neglect their dependence on x .
 - [20] V. A. Kholod and V. M. Yakovenko, Pis'ma ZhETF 77, 494 (2003) [JETP Lett. 77, 420 (2003)].
 - [21] F. Guinea, R. S. Markiewicz, and M. A. H. Vozmediano, Phys. Rev. B 69, 054509 (2004).
 - [22] A. A. Abrikosov, Phys. Rev. B 53, R8910 (1996).
 - [23] J. A. Skinta, T. R. Lemberger, T. Greibe, and M. Naito, Phys. Rev. Lett. 88, 207003 (2002).
 - [24] J. L. Peng, E. M. Aiser, T. Venkatesan, R. L. Greene, and G. Czjzek, Phys. Rev. B 55, R6145 (1997); A. Sawa, M. Kawasaki, H. Takagi, and Y. Tokura, Phys. Rev. B 66, 014531 (2002).
 - [25] D. Vollhardt and P. Wölfe, The Superfluid Phases of Helium 3 (Taylor and Francis, London, 1990).
 - [26] G. E. Volovik and L. P. Gor'kov, Zh. Eksp. Teor. Fiz. 88, 1412 (1985) [Sov. Phys. JETP 61, 843 (1985)]; M. Sigrist and K. Ueda, Rev. Mod. Phys. 63, 239 (1991).
 - [27] K. Miyake and O. Narikiyo, Phys. Rev. Lett. 83, 1423 (1999).
 - [28] K. Sengupta, H.-J. Kwon, and V. M. Yakovenko, Phys. Rev. B 65, 104504 (2002).
 - [29] G.-Q. Zheng, T. Sato, Y. Kitaoka, M. Fujita, and K. Yamada, Phys. Rev. Lett. 90, 197005 (2003).
 - [30] F. Zambrorsky, G. Wu, S. Dunsiger, E. Artukovic, J. Shinagawa, A. Lacerda, H. Baki, R. L. Greene, W. G. Clark, and S. E. Brown, unpublished.
 - [31] K. Ishida, H. Mukuda, Y. Kitaoka, K. Asayama, Z. Q. Mao, Y. Mori, and Y. Maeno, Nature 396, 658 (1998).
 - [32] I. J. Lee, S. E. Brown, W. G. Clark, M. J. Strouse, M. J. Naughton, W. Kang, and P. M. Chaikin, Phys. Rev. Lett. 88, 017004 (2002).
 - [33] J. E. Sonier, K. F. Poon, G. M. Luke, P. Kyriakou, R. I. Miller, R. Liang, C. R. Wiebe, P. Fournier, and R. L. Greene, Phys. Rev. Lett. 91, 147002 (2003).
 - [34] G. M. Luke, Y. Fudamoto, K. M. Kojima, M. I. Larkin, J. Merrin, B. Nachumi, Y. J. Uemura, Y. Maeno, Z. Q. Mao, Y. Mori, H. Nakamura, and M. Sigrist, Nature 394, 558 (1998).
 - [35] H.-J. Kwon, V. M. Yakovenko, and K. Sengupta, Synth. Met. 133-134, 27 (2003).
 - [36] R. C. Black, A. Mathai, F. C. Wellstood, E. Dantsker, A. H. Miklich, D. T. Nemeth, J. J. Kingston, and J. Clarke, Appl. Phys. Lett. 62, 2128 (1993); L. N. Vu, M. S. Wistrom, and D. J. Van Harlingen, Appl. Phys. Lett. 63, 1693 (1993); C. C. Tsuei, J. R. Kirtley, C. C. Chi, L. S. Yu-Jahnes, A. Gupta, T. Shaw, J. Z. Sun, and M. B. Ketchen, Phys. Rev. Lett. 73, 593 (1994); K. A. Moler, J. R. Kirtley, D. G. Hinks, T. W. Li, and M. Xu, Science 279, 1193 (1998).
 - [37] I. I. Mazin and D. J. Singh, Phys. Rev. Lett. 79, 733 (1997); 82, 4324 (1999).
 - [38] K. Kuboki, J. Phys. Soc. Jpn. 70, 2698 (2001).
 - [39] C. Castellani, D. Di Castro, and M. Grilli, Z. Phys. B 103, 137 (1997).
 - [40] A. Ino, C. Kim, M. Nakamura, T. Yoshida, T. Mizokawa, A. Fujimori, Z.-X. Shen, T. Kakeshita, H. Eisaki, and S. Uchida, Phys. Rev. B 65, 094504 (2002).
 - [41] H. Baki and R. L. Greene, cond-mat/0402263.
 - [42] U. M. Scheven, E. I. Chashchikina, E. Lee, and P. M. Chaikin, Phys. Rev. B 52, 3484 (1995).
 - [43] M. Voja, Y. Zhang, and S. Sachdev, Phys. Rev. Lett. 85, 4940 (2000).
 - [44] J. W. Clark, V. A. Kholod, M. V. Zverev, and V. M. Yakovenko, Phys. Rep. 391, 123 (2004).
 - [45] C. Honerkamp, Eur. Phys. J. B 21, 81 (2001).
 - [46] B. Kyung, J.-S. Landry, and A.-M. S. Tremblay, Phys. Rev. B 68, 174502 (2003).